The Astrophysical Journal Letters, 839:L1 (6pp), 2017 April 10 https://doi.org/10.3847/2041-8213/aa693a

Assessing the Habitability of the TRAPPIST-1 System Using a 3D Climate Model

Eric T. Wolf
Laboratory for Atmospheric and Space Physics, Department of Atmospheric and Oceanic Sciences, University of Colorado, Boulder, CO, USA; eric.wolf@colorado.edu
Received 2017 March 16; revised 2017 March 24; accepted 2017 March 24; published 2017 April 6

Abstract

The TRAPPIST-1 system provides an extraordinary opportunity to study multiple terrestrial extrasolar planets and their atmospheres. Here, we use the National Center for Atmospheric Research Community Atmosphere Model version 4 to study the possible climate and habitability of the planets in the TRAPPIST-1 system. We assume the worlds are ocean-covered, with atmospheres composed of N_2, CO_2, and H_2O, and with orbital and geophysical properties defined from observation. Model results indicate that the inner three planets (b, c, and d) presently reside interior to the inner edge of the traditional liquid water habitable zone. Thus, if water ever existed on the inner planets, they would have undergone a runaway greenhouse and lost their water to space, leaving them dry today. Conversely, the outer three planets (f, g, and h) fall beyond the maximum CO_2 greenhouse outer edge of the habitable zone. Model results indicate that the outer planets cannot be warmed, despite having as much as 30 bar CO_2 atmospheres, instead entering a snowball state. The middle planet (e) represents the best chance for a presently habitable ocean-covered world in the TRAPPIST-1 system. Planet e can maintain at least some habitable surface area with 0–2 bar CO_2, depending on the background N_2 content. Near-present-day Earth surface temperatures can be maintained for an ocean-covered planet e with either 1 bar N_2 + 0.4 bar CO_2, or a 1.3 bar pure CO_2 atmosphere.

Key words: astrobiology – planets and satellites: atmospheres – planets and satellites: terrestrial planets

1. Introduction

Recently, seven planets were found orbiting the ultracool star TRAPPIST-1 in a transiting configuration (Gillon et al. 2016, 2017). These seven planets are remarkable because they are all terrestrial sized, with masses ranging from 0.41 to 1.38 $M_\oplus$ and radii ranging from 0.755 to 1.086 $R_\oplus$. These planets receive relative incident stellar fluxes of 0.131–4.24 $S/S_\oplus$, where $S_\oplus$ is the total stellar flux received by the modern Earth (~1360 Wm^{-2}). The transiting configuration of these planets means that current and future missions can attempt to characterize their atmospheres through transit spectroscopy. Thus, the TRAPPIST-1 system will provide the community new ground where theory on the evolution of terrestrial planet atmospheres can be tested against observations. Gillon et al. (2017) suggest that the seven TRAPPIST-1 planets may be "temperate" because all have equilibrium temperatures below ~400 K. However, equilibrium temperature is a rudimentary metric of planetary climate. Equilibrium temperature ignores the greenhouse effect, while the albedo is generally unknown. To obtain an improved assessment of habitability for the TRAPPIST-1 planets, one must use advanced climate models that can adequately compute the greenhouse effect, planetary albedo, and ultimately the surface temperature.

Earth provides the only archetype for a robustly habitable world. Thus, by definition, habitable planets must maintain generically Earth-like surface conditions, with abundantly available liquid water (Hart 1979). The necessary condition of surface liquid water implies a surface temperature range of 273–373 K. However, despite our Earth-centric definition for planetary habitability, TRAPPIST-1 and its planetary system are quite different from our own. TRAPPIST-1 is an ultracool dwarf star, meaning that it is small, dim, and red. Each of these factors has important consequences for the potential climates of its seven orbiting planets. TRAPPIST-1 has a mass of only 0.08 $M_\odot$ and a luminosity of only 5.25×10^{-4} $L_\odot$ (Gillon et al. 2016). Thus, despite all seven planets orbiting within 0.063 au from the star, they receive a moderate range of incident stellar radiation. However, their close-in orbits mean that all planets in the system are likely locked into tidal synchronization, particularly given their low eccentricities (Gillon et al. 2017). Thus, one side of the planet always faces the star, and the planetary rotational period equals the orbital period. Generally, tidal locking implies planetary rotation rates that are slower than Earth's, and this holds true for the TRAPPIST-1 system. However, the orbital periods for planets b–f are less than ~10 Earth days. Thus, even if synchronously rotating, the Coriolis effect will be non-negligible and these worlds retain zonal flow patterns (Kopparapu et al. 2016). TRAPPIST-1 is quite cool, with an effective temperature of only ~2560 K. Thus, its emitted stellar radiation is shifted toward the near-infrared compared with our Sun. This shift affects radiative interactions in the atmosphere and with the surface because near-infrared radiation is more readily absorbed by water vapor and sea ice (Shields et al. 2013). With these characteristics of the star–planet system in mind, we conduct 3D climate calculations for planets in the TRAPPIST-1 system assuming atmospheres composed of N_2, CO_2, and H_2O, following the traditional assumptions for terrestrial planetary atmospheres within the habitable zone (Kasting et al. 1993; Selsis et al. 2007; Kopparapu et al. 2013).

2. Methods

We use a modified version of the Community Atmosphere Model (Neale et al. 2010) version 4 (CAM4) from the National Center for Atmospheric Research. We have used this particular model version previously for studying a variety of Earth-like atmospheres (Wolf & Toon 2013, 2014a, 2014b, 2015; Wolf et al. 2017), and CAM4 has been frequently used elsewhere for studying slow rotating planets around M-dwarf stars (Yang et al. 2013, 2014; Kopparapu et al. 2016; Wang et al. 2016). We have modified the radiative transfer code in the model (e.g.,

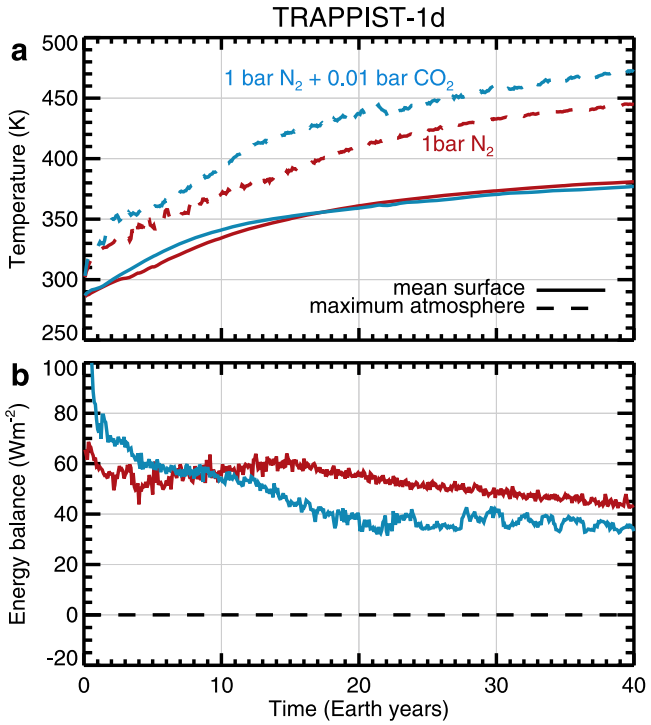

Figure 1. Time series model outputs from simulations of TRAPPIST-1d with atmospheric compositions of 1 bar N_2 and 1 bar N_2 + 0.01 bar CO_2. The top panel (a) shows the mean surface and maximum atmosphere temperatures. The bottom panel (b) shows the top-of-atmosphere energy imbalance.

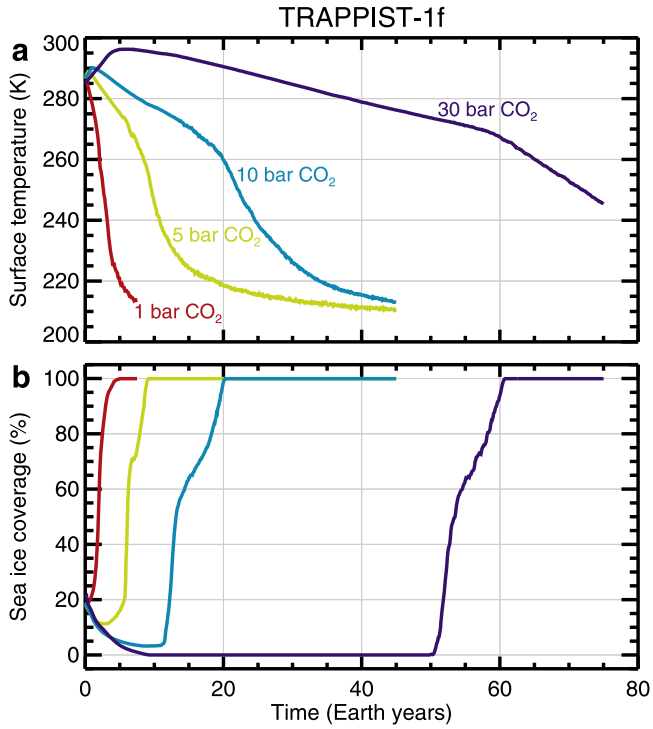

Figure 2. Time series model outputs from simulations of TRAPPIST-1f with dense CO_2 atmospheres. The top panel (a) shows the mean surface temperatures. The bottom panel (b) shows percent sea-ice coverage.

Wolf & Toon 2013) and have also incorporated new methods to improve the numerical stability of the model for these exotic atmospheres. We use the planetary masses, radii, and surface gravity determined from observations (Gillon et al. 2017, Table 1). We assume that all planets are locked into synchronous rotation (i.e., a 1:1 spin–orbit ratio), thus their rotational period is equal to their orbital period. We assume the planet is completely ocean-covered, with zero ocean heat transport within a 50 m thermodynamic slab ocean (Bitz et al. 2012). Sea ice forms wherever the sea surface temperature falls below the freezing point of seawater (−1.8°C in the model). We use $4^\circ \times 5^\circ$ horizontal resolution with 40 vertical levels extending from the surface up to a 1 mb model top. Clouds and convection use the subgrid-scale parameterizations of Rasch & Kristjánsson (1998) and Zhang & McFarlane (1995), respectively. We use the incident stellar spectra from the BT_Settl stellar models for a 2600 K star (Allard et al. 2003, 2007). We assume several basic atmospheric compositions; $N_2 + H_2O$, $N_2 + CO_2 + H_2O$, and finally $CO_2 + H_2O$. We conduct simulations for planets d, e, and f, which lie at the center of the TRAPPIST-1 system. As described below, the habitability of planets b and c can be inferred from results for planet d. Likewise, the habitability of planets g and h can be inferred from results for planet f.

3. Results

Figure 1 shows a time series of 3D climate model results for global mean surface temperature (T_s) and top-of-atmosphere energy balance for simulations of planet d. Planet d receives an incident stellar flux of 1.143 $S/S_\oplus$, with a 4.05 Earth-day period. With 1 bar N_2 and no greenhouse gases (other than H_2O), the climate undergoes a thermal runaway and becomes uninhabitable. In Figure 1, simulations were run for 40 years. At that point, $T_s \sim 380$ K, the maximum temperature of the atmosphere exceeds ∼450 K, and a large (∼40 Wm^{-2}) residual top-of-atmosphere energy imbalance remains, indicating further warming would occur if the simulation continued. Note also that when $T_s \sim 380$ K, the total atmospheric pressure has doubled because now the atmosphere contains ∼1 bar of H_2O in addition to its dry constituents. These water-dominated atmospheres could lose an Earth-ocean of water to space in only several million years at the diffusion-limited rate (Hunten 1973). Thus, planet d is most likely hot, dry, and uninhabitable today.

We do not explicitly simulate planets b and c here. They receive stellar fluxes of 2.27 and 4.25 $S/S_\oplus$, respectively, and thus they would be significantly hotter than planet d, given identical atmospheric compositions and surface characteristics. Thus, planets b, c, and d reside interior to the traditional liquid water habitable zone. This diagnosis is in agreement with the habitable zone limits of Kopparapu et al. (2013) for low-mass stars and also preliminary assessments of the system by Gillon et al. (2017). However, some studies have suggested that locally habitable conditions may exist on dry (i.e., water-limited) planets that lie interior to the traditional habitable zone (Abe et al. 2011; Leconte et al. 2013a).

Conversely, simulations of planet f cannot be prevented from entering a completely ice-covered state despite dense CO_2 atmospheres (Figure 2). Planet f receives only 0.382 $S/S_\oplus$ with a 9.21 Earth-day period. Here, we find that even with 30 bars of CO_2, planet f would be completely ice covered. Furthermore, for all simulations of planet f (Figure 2), temperatures become cold enough that CO_2 would condense onto the surface, and thus these atmospheres would collapse. Planets g and h receive

0.258 and 0.131 $S/S_{\oplus}$, respectively. While we do not explicitly simulate these worlds, they receive considerably less stellar flux than planet f does, and thus they too would be unable to escape a snowball state if warmed by CO_2 alone. Thus, we conclude that planets f, g, and h lie outside the traditional liquid water habitable zone defined by the maximum CO_2 greenhouse limit.

Note that the 1D modeling study of Kopparapu et al. (2013) suggests that planets f and g may fall within the maximum CO_2 greenhouse limit; however, they make several assumptions in their model that lead to warmer planets. First, they neglect increases to the surface albedo due to expanding sea ice and snow. Second, they ignore increases to the planetary albedo due to the formation of thick substellar clouds on synchronous rotators (Yang et al. 2013; Kopparapu et al. 2016). Finally, they assume that the atmosphere is saturated with respect to water vapor, artificially maximizing the greenhouse effect. Thus, the Kopparapu et al. (2013) results may be overly generous with respect to the maximum CO_2 greenhouse limit for the outer edge of the habitable zone. However, others have suggested that H_2 could play a significant role in warming planets at low stellar fluxes (e.g., Pierrehumbert & Gaidos 2011).

Planet e, the central planet in the system, provides the most viable candidate for a robustly habitable world. Figure 3(a) shows results for the global mean surface temperature of planet e, for simulations with a 1 bar N_2 background and varying CO_2 (red), and also for pure CO_2 atmospheres (blue). Figure 3(b) shows the global mean percent sea-ice coverage. Figure 3(c) shows the percent of habitable surface area. The habitable area is defined as the percent of the planet's surface that is both ice free and has a surface temperature less than 310 K. While some life forms on Earth survive at hotter surface temperatures or in glaciated areas, this range of surface conditions (approximately) encompasses the limits for human biological functioning unaided by technology (Sherwood & Huber 2010).

Simulations indicate that planet e can maintain habitable surface conditions for a variety of atmospheric compositions. Planet e receives only 0.662 $S/S_{\oplus}$ with a 6.10 Earth-day period. Thus, without additional greenhouse gases, planet e would be cold. However, even with thin atmospheres, planet e can remain habitable locally at the substellar point. With 1 bar N_2 and zero CO_2 (not shown in Figure 3), $T_s \sim 227$ K, and a small part of the ocean (~13%) remains thawed immediately around the substellar point, with temperatures hovering near ~280 K locally. Marginally warmer conditions are found with an Earth-like composition (1 bar N_2 + 10^{-4} bar CO_2) and also in the case of a thin pure CO_2 atmosphere with a surface pressure of only 0.25 bar. These cases have $T_s \sim 240$ K, sea-ice coverage of ~80%, while ~20% of the planet surface is habitable.

Global mean surface temperatures near those of present-day Earth (~288 K) can be maintained on planet e presently with either 1 bar N_2 + 0.4 bar CO_2, or similarly by 1.3 bar CO_2. Perhaps coincidentally, an Earth-like temperature coincides with maxima in the habitable surface area (>95%) with ice confined to the poles and moderate surface temperatures elsewhere. However, for further increasing CO_2 amounts, the habitable surface area sharply declines as surface temperatures locally warm beyond the human heat stress limit (Sherwood & Huber 2010). The habitable area eventually falls to zero for atmospheric compositions of 1 bar N_2 + 2 bar CO_2, and similarly for 4 bar CO_2. These hot but stable states have $T_s \geqslant 330$ K. However, their stratospheric H_2O volume mixing ratios remain small (~10^{-5} at 1 mb) due to efficient cold trapping caused by cooling of the middle and upper atmosphere from high CO_2 concentrations (e.g., Wordsworth & Pierrehumbert 2013). Thus, while the runaway cases described in Figure 1 would cause planets b, c, and d to be desiccated today, planets with hot stable climates shown in Figure 3 could retain their water for long periods of time.

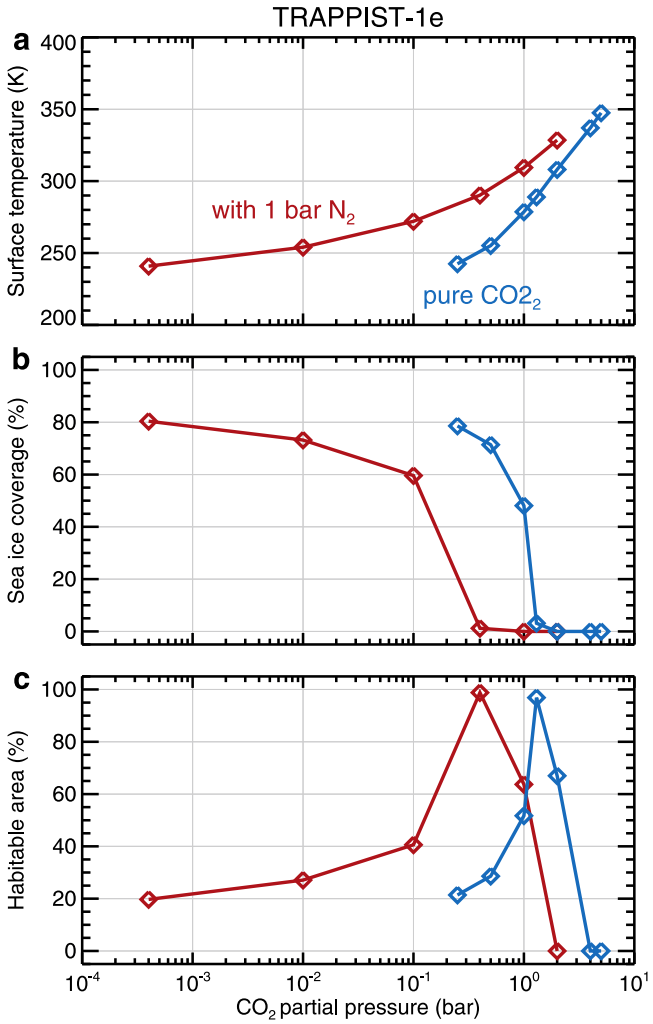

Figure 3. Simulations of TRAPPIST-1e with a various atmospheric compositions. All simulations shown are in equilibrium. Shown are the mean surface temperature (a), the sea-ice coverage (b), and the habitable surface area (c). Red lines indicate simulations containing a 1 bar N_2 background, plus additional CO_2. Blue lines indicate simulations containing a pure CO_2 atmosphere. All simulations include H_2O.

Figure 4 shows the temporal mean surface temperature, cloud water column, net outgoing thermal radiation, and reflected stellar radiation from the primary atmospheric states studied here: a completely glaciated "snowball" planet f, a "cold" but marginally habitable planet e, a "temperate" planet e at modern Earth temperatures, a "hot" and uninhabitable planet e, and finally an incipient thermal "runaway" for planet d. Descriptions of each simulation are in the left margin of Figure 4. In surface temperature contour maps, solid white lines indicate the sea-ice margin, and dashed white lines indicate where CO_2 would condense onto the surface of the planet. The substellar point is located at the center of each frame. Note that the runaway case will continue to increase in temperature beyond what is illustrated and would eventually lose its water

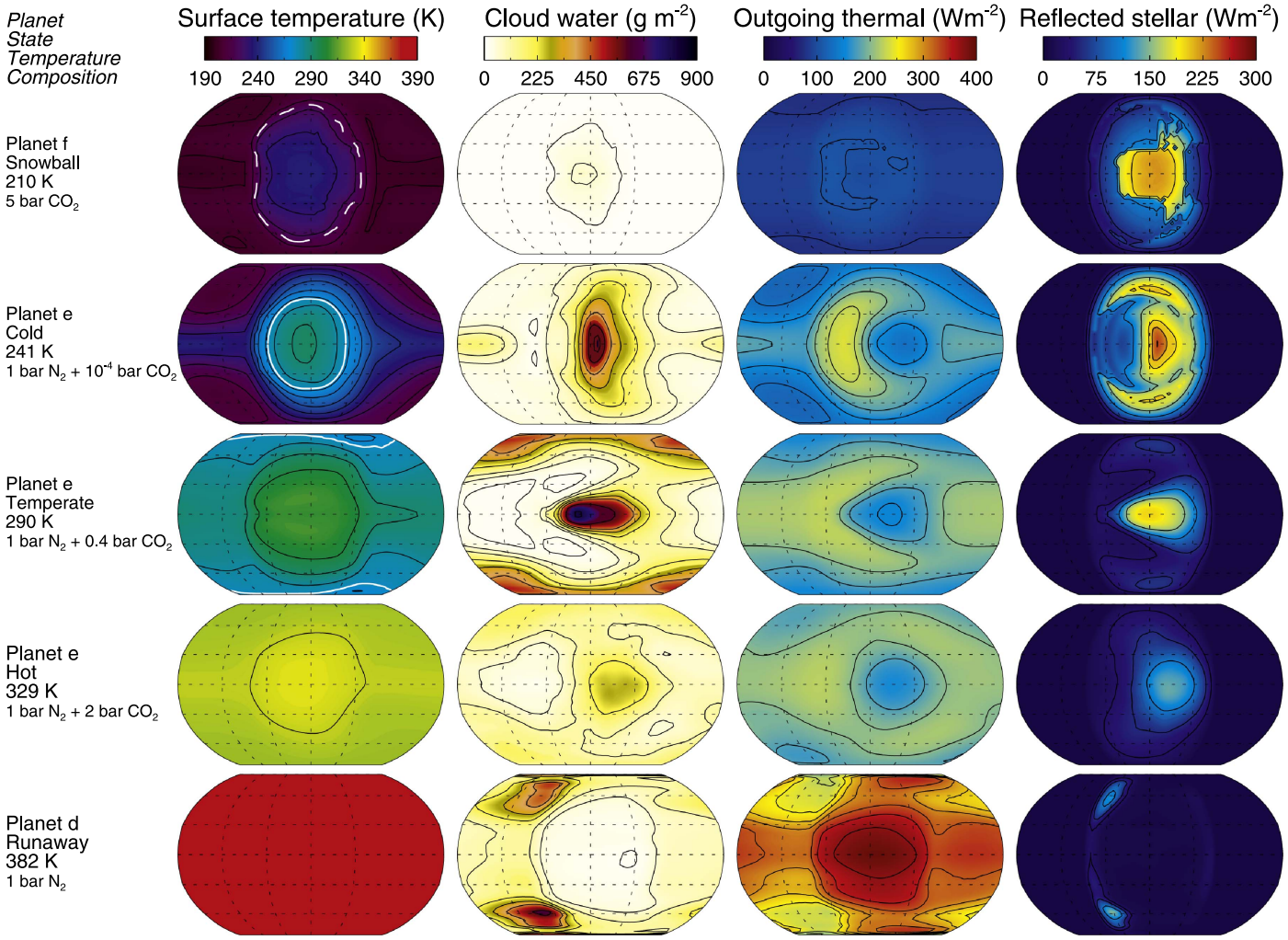

Figure 4. Contour plots of surface temperature, cloud water column, net outgoing thermal flux, and reflected stellar flux for several atmosphere types, including snowball, cold, temperate, hot, and runaway. Note the description of each simulation in the left-hand margin of the figure. In the surface temperature maps, a white solid line indicates the sea-ice margin and a dashed white line indicates CO_2 condensation onto the surface.

to space. Thus, the image of a runaway shown is a snapshot of a transient state.

The snowball planet f is completely covered in ice and has minimal clouds and water vapor in its atmosphere. The thermal emitted flux is low due to its cold temperature, but the reflected stellar energy is significant due to snow and ice cover. Though not explicitly included in the model, the atmosphere is cold enough that CO_2 would condense onto the night side of the planet, causing the atmosphere to collapse. The cold planet e can maintain open ocean only immediately around the substellar point, but the majority of the planet is ice covered. Thick clouds form over open waters at the substellar point and contribute significantly to the planetary energy balance by increasing the albedo and decreasing the emitted thermal flux where clouds are thickest. This pattern is also seen in warmer cases. For the cold planet e, sea ice also contributes to the reflected stellar energy near the terminators. A temperate planet e is the most favorable scenario and maintains habitable conditions over virtually its entire surface. Sea ice is confined to the poles. Clouds are thick over the substellar point and poles, and the thermal and reflected flux fields mirror the distribution of the clouds. The final two states are increasingly hot and uninhabitable. As climate warms, surface temperatures become uniform across the planet and sea ice vanishes entirely. Despite significant water vapor in their atmospheres, relative humidity and clouds decrease for hot atmospheres. For increasing temperatures, the day side becomes increasingly dry (i.e., low relative humidity) and substellar clouds thin and eventually vanish. In the runaway case, clouds can only be maintained on the night side and along the terminator. The reduction in day side clouds reduces the amount of reflected stellar energy from these hot worlds. The outgoing thermal flux for the hot case is comparable to that of the temperate case; however, the outgoing thermal flux becomes large for an atmosphere in runaway.

The net outgoing thermal and reflected stellar flux maps shown in Figure 4 begin to tell us how these climate states may appear to the distant observer. From these flux maps, it is helpful to construct phase curves (e.g., Koll & Abbot 2015, Appendix C) of the thermal emitted flux and the planetary albedo (Figure 5). Note that at a phase angle of 0° the observer sees the day side of the planet, and at phase angles of −180° and 180° the observer sees the night side of the planet. From phase curves, one can distinguish between atmospheres of interest. An incipient thermal runaway emits between 300 and 400 Wm^{-2} of thermal flux, due to its hot and sub-saturated atmosphere. However, its albedo is small and near zero at a phase angle of 0°. The thermal emitted flux and albedo are out

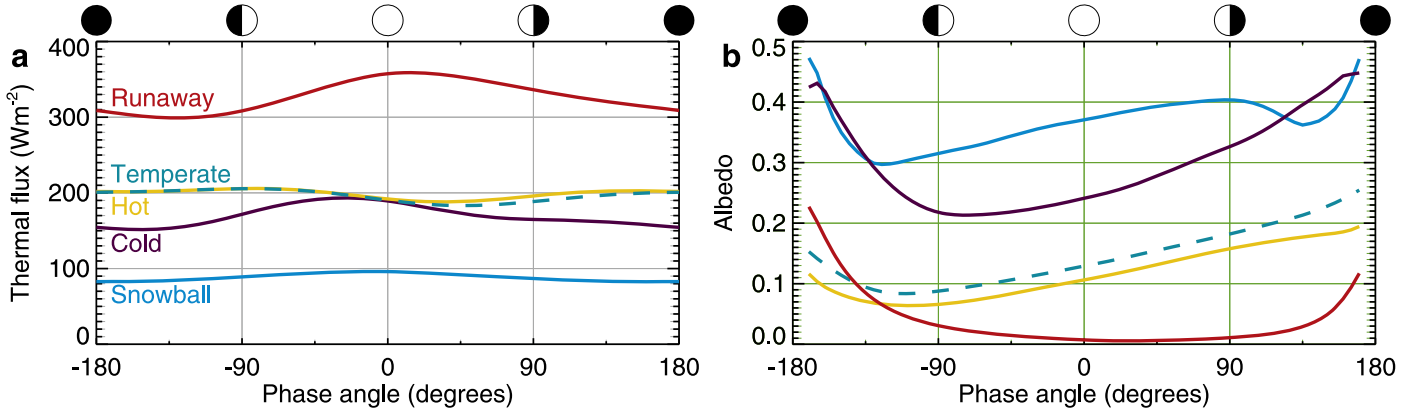

Figure 5. Phase curves of emitted thermal flux and planetary albedo based on the simulations shown in Figure 4.

of phase, with maximum emission occurring at a phase angle of 0° concurrent with the minimum in albedo. The albedo increases near −180° and 180° due to grazing incidence scattering from clouds found along the terminator regions. Note that grazing incidence causes the albedo to increase at phase angles near −180° and 180° for all cases.

The snowball case can be distinguished by having a low emitted thermal flux (<100 Wm^{-2}), while also featuring the highest albedo. We find the albedo to range between 0.3 and 0.5. Temperate, and hot climates are more difficult to distinguish from each other. Their emitted thermal phase curves are virtually identical (∼200 Wm^{-2}), despite a ∼40 K difference in T_s. The albedo of the hot climate is about ∼20% lower than that of the temperate climate. Finally, the cold case emits slightly less thermal flux (∼150–200 Wm^{-2}), with a maximum found at a phase angle of 0° and is out of phase with the hot and temperate cases. The albedo of the cold case is significantly greater than that of both hot and temperate cases; however, it is less than the snowball case.

4. Conclusions

Here, we have used a state-of-the-art 3D climate system model to take a first cut at evaluating the climate and habitability of the TRAPPIST-1 system. Planets b, c, and d are likely too hot to support abundant liquid water at their surfaces. These planets would have undergone a runaway greenhouse process and have probably lost their water to space long ago. Planets f, g, and h are likely too cold to support surface liquid water. If these planets contain water, they are probably encased in ice and snow, despite as much as 30 bars of CO_2. Planet e is the best chance for a presently habitable ocean-covered world in the TRAPPIST-1 system. Planet e can maintain at least some habitable surface area under a variety of atmospheric compositions. With a 1 bar N_2 background, planet e is habitable for CO_2 amounts up to 1 bar. For pure CO_2 atmospheres, planet e is habitable with CO_2 ranging from 0.25–2 bars. Planet e can maintain near-present-day Earth surface temperatures with a 1.3 bar pure CO_2 atmosphere, or 1 bar N_2 + 0.4 bar CO_2.

However, these simulations are predicated on the assumption that each planet has abundant surface water at their present time and location in the system. The super-luminous pre-main-sequence phase of low-mass stars may spell doom for planets orbiting in their habitable zones today (Luger & Barnes 2015). Ultracool dwarf stars may take up to ∼1 Gyr to settle onto the main sequence, subjecting any planets to intense stellar radiation, driving them into runaway greenhouse conditions. Bolmont et al. (2016) predict that planet d, given its confirmed location in the system at 0.021 au, may have lost up to ∼7 Earth oceans of water. While planet e had not been identified at the time of the study, the Bolmont et al. (2016) results indicate that planet e may have lost several Earth oceans of water during the pre-main-sequence phase. Thus, planet e would have needed an initial water inventory at least several times greater than the Earth currently has for it to retain abundant water today. An alternative idea is that the TRAPPIST-1 planets may have formed further out and then migrated to their current positions (Terquem & Papaloizou 2007), thus circumventing the pre-main-sequence runaway phase, and making it easier from them to retain primordial volatiles. Additionally, it has been suggested that surface-mantle volatile cycling may not reach equilibrium until several Gyr after planetary formation, and thus surface water could be replenished from the interior after the pre-main-sequence phase concludes (Komacek & Abbot 2016).

It is also important to note that these simulations originate from a single 3D climate system model. Differences among climate models exist, particularly for exoplanetary problems that push the boundaries of these originally Earth-centric codes (e.g., Leconte et al. 2013b; Wolf & Toon 2015; Popp et al. 2016). Gillon et al. (2017) assert that 3D climate model simulations of terrestrial planets around low-mass stars (e.g., Turbet et al. 2016) indicate that planets b, c, and d would undergo a runaway greenhouse, while planets e, f, and g could be habitable given "Earth-like" atmospheres. While our results agree regarding planets b, c, and d, in this study planets f and g are too cold to be habitable. Surely, future works will examine the climate and habitability of the TRAPPIST-1 planets using a variety of 1D and 3D atmosphere models. Through careful model intercomparison, we can gain confidence in our ability to simulate the climates of the TRAPPIST-1 system.

E.T.W. acknowledges support from NASA Planetary Atmospheres Program award NNX14AH17G and from the NASA Habitable Worlds program award NNX16AB61G. This work utilized the Janus supercomputer, which is supported by the National Science Foundation (award CNS-0821794) and the University of Colorado at Boulder. This work was also facilitated through the use of advanced computational, storage, and networking infrastructure provided by the Hyak supercomputer system, supported in part by the University of Washington eScience Institute. E.T.W. thanks the NASA

Astrobiology Institute's Virtual Planetary Laboratory at the University of Washington for granting computing time on Hyak. E.T.W. also thanks D. S. Abbot, R. K. Kopparapu, J. Haqq-Misra, and O. B. Toon for helpful comments and discussions.

References

Abe, Y., Abe-Ouchi, A., Sleep, N. H., & Zahnle, K. J. 2011, AsBio, 11, 443
Allard, F., Allard, N. F., Homeier, D., et al. 2007, A&A, 474, L21
Allard, F., Guillot, T., Ludwig, H. G., et al. 2003, in IAU Symp. 211, Brown Dwarfs, ed. E. Martín (San Francisco, CA: ASP), 325
Bitz, C. M., Shell, K. M., Gent, P. R., et al. 2012, JCli, 25, 3053
Bolmont, E., Selsis, F., Owen, J. E., et al. 2016, MNRAS, 464, 3728
Gillon, M., Jehin, E., Lederer, S. M., et al. 2016, Natur, 533, 221
Gillon, M., Triaud, A. H. M. J., Demory, B.-O., et al. 2017, Natur, 542, 456
Hart, M. H. 1979, Icar, 37, 35
Hunten, D. M. 1973, JAtS, 30, 1481
Kasting, J. F., Whitmire, D. P., & Reynolds, R. T. 1993, Icar, 101, 108
Koll, D. D. B., & Abbot, D. S. 2015, ApJ, 802, 21
Komacek, T. D., & Abbot, D. S. 2016, ApJ, 832, 54
Kopparapu, R. K., Ramirez, R., Kasting, J. F., et al. 2013, ApJ, 765, 131
Kopparapu, R. K., Wolf, E. T., Haqq-Misra, J., et al. 2016, ApJ, 819, 84
Leconte, J., Forget, F., Charnay, B., et al. 2013a, A&A, 554, A69
Leconte, J., Forget, F., Charnay, B., et al. 2013b, Natur, 504, 268
Luger, R., & Barnes, R. 2015, AsBio, 15, 119
Neale, R. B., Richter, J. H., Conley, A. J., et al. 2010, NCAR Technical Note, NCAR/TN-486+STR, http://www.cesm.ucar.edu/models/ccsm4.0/cam/docs/description/cam4_desc.pdf
Pierrehumbert, R., & Gaidos, E. 2011, ApJL, 734, L13
Popp, M., Schmidt, H., & Marotzke, J. 2016, NatCo, 7, 10627
Rasch, P. J., & Kristjánsson, J. E. 1998, JCli, 11, 1587
Selsis, F., Kasting, J. F., Levrard, B., et al. 2007, A&A, 476, 1373
Sherwood, S. C., & Huber, M. 2010, PNAS, 107, 9552
Shields, A. L., Meadows, V. S., Bitz, C. M., et al. 2013, AsBio, 13, 715
Terquem, C., & Papaloizou, J. C. B. 2007, ApJ, 654, 1110
Turbet, M., Leconte, J., Selsis, F., et al. 2016, A&A, 596, A112
Wang, Y., Liu, Y., Tian, F., et al. 2016, ApJL, 823, L20
Wolf, E. T., Shields, A. L., Kopparapu, R. K., et al. 2017, ApJ, 837, 107
Wolf, E. T., & Toon, O. B. 2013, AsBio, 13, 1
Wolf, E. T., & Toon, O. B. 2014a, GeoRL, 41, 167
Wolf, E. T., & Toon, O. B. 2014b, AsBio, 14, 241
Wolf, E. T., & Toon, O. B. 2015, JGRD, 120, 5775
Wordsworth, R. D., & Pierrehumbert, R. T. 2013, ApJ, 778, 154
Yang, J., Boué, G., Fabrycky, D. C., & Abbot, D. S. 2014, ApJL, 787, L2
Yang, J., Cowan, N. B., & Abbot, D. S. 2013, ApJL, 771, L45
Zhang, G. J., & McFarlane, N. A. 1995, AtO, 33, 407